Eur J Nutr (2013) 52:1067–1075
DOI 10.1007/s00394-012-0413-6

ORIGINAL CONTRIBUTION

Octreotide alleviates obesity by reducing intestinal glucose absorption and inhibiting low-grade inflammation

R. Liu · N. Wei · W. Guo · O. Qiang · X. Li · Y. Ou · W. Huang · C. W. Tang

Received: 19 January 2012 / Accepted: 27 June 2012 / Published online: 18 July 2012

Abstract
Purpose To investigate the role of octreotide, a somatostatin (SST) analog with anti-inflammatory effects, on the digestive and absorptive functions of jejunum in rats fed a high-fat diet, as well as its therapeutic prospects for diet-induced obesity.
Methods Rats were divided into three groups with different diet and treatment for the 176-day experiment: (1) control, 18 rats fed with standard chow, (2) high-fat control, 19 rats fed with high-fat chow, and (3) high-fat octreotide, 21 rats fed with high-fat chow and treated with octreotide for the last 8 days of the experiment. Plasma tumor necrosis factor-α (TNF-α) was measured by ELISA and SST by radioimmunoassay. Disaccharidase activity in the jejunal homogenate was determined. SST and Na^+-dependent glucose transporter 1 (SGLT-1) in the jejunal mucosa were visualized by immunohistochemistry. SGLT-1 was quantified by reverse transcription polymerase chain reaction and Western blot assays.
Results After 176 days, the fat/body weight ratio, villus height, maltase, SGLT-1, and plasma TNF-α in the high-fat control rats were much higher than those in the control rats ($p < 0.01$ or $p < 0.05$) and were significantly lower in the high-fat + octreotide rats ($p < 0.01$ or $p < 0.05$). SST levels were dramatically different in the intestinal mucosa of the two high-fat groups (231.12 ± 98.18 pg/mg in the high-fat controls and 480.01 ± 286.65 pg/mg in the octreotide group).
Conclusions The low-grade inflammation induced by high-fat diet apparently reduced the secretion of intestinal SST, which increased intestinal absorption of energy and nutrients and formation of adipose tissues. Octreotide effectively reversed this process, a finding that has far-reaching significance for the regulation of energy balance.

Keywords Obesity · Jejunal absorption · Octreotide · Na^+-dependent glucose transporter protein (SGLT-1) · Maltase · Rat

R. Liu (✉) · N. Wei · W. Guo · O. Qiang · X. Li · Y. Ou · W. Huang · C. W. Tang (✉)
Division of Peptides Related with Human Disease, State Key Laboratory of Biotherapy, West China Hospital, Sichuan University, Chengdu 610041, People's Republic of China
e-mail: lrui60@yahoo.com.cn

C. W. Tang
e-mail: shcqcdmed@163.com

N. Wei · Y. Ou · W. Huang · C. W. Tang
Department of Gastroenterology, West China Hospital, Sichuan University, Chengdu 610041, People's Republic of China

Introduction

Obesity is quickly becoming a worldwide epidemic, one with important adverse medical, psychosocial, and economic consequences [1]. Strategies such as diet restriction, exercise, and behavioral therapy are only modestly effective in treating obesity, especially in the long term. Although gastric bypass surgery has been widely performed [2], this procedure carries significant risks. Very few weight reduction drugs have been approved, and their effects are also limited [3].

Somatostatin (SST), a 14- or 28-amino-acid peptide hormone with extensive biological activity, is widely distributed in the gastrointestinal tract and central nervous system. SST and its analogs (SSTA, such as octreotide and lanreotide) bind to SST subtype 5 receptors (SSTR-5) on the β-cell membrane, which limits insulin release and, consequently, may decrease adipogenesis [4]. SSTA has been used in trials in patients with pediatric hypothalamic

obesity [5]. However, its application for diet-induced obesity has not been systematically investigated.

Recent studies have revealed a close relationship between inflammatory and metabolic pathways [6]. Considerable attention is being paid to the distal gut, where microbiota may affect metabolic diseases by activating the innate immune system [6]. The link between inflammation, adipose tissue metabolism, and plasticity is not fully understood. One clue is that gut microbiota has been shown to determine adipose tissue physiology through lipopolysaccharide (LPS)–endocannabinoid system regulatory loops, and may have critical functions in adipose tissue plasticity in obesity [7]. However, the gut barrier alterations described in those animal models of obesity have not been found in obese humans [8].

The small intestine is the major place where the carbohydrate is digested and absorbed. Disaccharidases, such as maltase and sucrase, are located mainly at the top of brush border of intestinal villi and play a crucial role in starch digestion [9]. The intestine modulates its glucose-absorptive capacity through changes in the expression of the intestinal sodium/glucose co-transporter 1 (SGLT-1), which transports dietary sugars from the lumen of the intestine into enterocytes at the intestinal brush border [10]. The change in the absorption area for jejunum likely influences the extent of digestion and absorption. Surgical resection of part of the intestine has been proposed for nutritional obesity, but is not widely accepted because of insufficient evidence-based data, potential complications including surgical morbidity and mortality, malabsorption, and absence of long-term safety data. Moreover, the small intestine is an important endocrine organ in the body [11]. It is not clear how the jejunal compartment reacts to the gut microbiota alterations that occur in obesity.

Our and other previous studies have revealed that SST and SSTA are important anti-inflammatory peptides in multiple pathways, acting as suppressors of the toll-like receptor 4 (TLR4)–nuclear factor κB (NF-κB) cytokine pathway and of intestinal mucosal mast cell (IMMC) activity, and inhibiting the function of various cell types that produce pro-inflammatory mediators [12–14]. Moreover, they are primary inhibitors of growth hormone and are negative regulators for intestinal epithelial growth [15–17]. This study aimed to identify the effects of octreotide, a type of SSTA, on the digestive and absorptive functions of jejunum in rats fed with high-fat diet, as well as its potential as a treatment for diet-induced obesity.

Methods

Animal and experimental grouping

Eighty healthy, male 21-day-old Sprague–Dawley (SD) rats obtained from the Animal Center of Sichuan University were allowed to acclimate and were adaptively fed with standard chow (290 kcal/100 g, in line with the People's Republic of China National Standard GB 14924-2001) for 3 days in the Animal Center of West China Hospital before the experiment. Then, the rats were randomized into two groups: one group of 20 was continuously fed the above-mentioned standard chow for 176 days as a normal control group, while another group of 60 was fed with high-fat chow (430 kcal/100 g). Food and water were supplied ad libitum; the rats were housed in independently ventilated animal cages on a 12:12-h light/dark schedule and kept at 20–25 °C. Their weights and body and tail lengths were measured weekly during the next 24 weeks' feeding. At the end of that time, rats with a mean body weight at least 1.4 times that of the controls were selected to continue the experiment. Forty eligible rats weighing 550–650 g were randomized into two groups: 19 in a high-fat control group and 21 in a high-fat + octreotide group. Both groups were continuously fed high-fat chow for 176 days, but the latter group was also subcutaneously injected with octreotide (40 μg/kg body weight) twice daily for the last 8 days of the experiment. The dosage of octreotide used in this study is within the typical range used by similar studies [18, 19]. All rats were measured weekly to calculate Lee's index [body weight $(g)^{1/3} \times 1{,}000$/body length (cm)].

At the end of the experiment, the rats were fasted for 12 h and killed with 2 % sodium pentobarbital given intraperitoneally. About 10-cm jejunal sections 2 cm away from the pylorus were quickly removed. Segments of proximal jejunum were weighed, and the mucosa was scraped with a glass slide and stored at −80 °C for the determination of disaccharidase activity, SGLT-1 expression, and SST level. The perirenal, testicular, and omental adipose tissues were collected and weighed for total fat content.

This study has been approved by the local Research Ethics Committee [REF: SYXK (Sichuan) 2008-119].

Morphological evaluation of the jejunal mucosa

Specimens of distal jejunum were fixed with 4 % paraformaldehyde (pH 7.4). The paraffin sections (5 μm) were stained with hematoxylin and eosin (HE) for histological evaluation. Using a microscope (DP-70 graphic analysis system, Olympus Corp., Tokyo, Japan), the number of villi per field of 40× magnification was counted and the height and crypt depth of 10 villi were measured. Other small jejunal specimens were immersed in 3 % glutaraldehyde (pH 7.4) at 4 °C for 24 h. Then, the specimens were postfixed in 1 % osmium tetroxide for 1 h and embedded in Epon812 after dehydration. Ultrathin sections (60 nm) were stained with uranyl acetate and lead citrate and

examined using a Hitachi H-600 IV transmission electron microscope (TEM; Hitachi Ltd., Tokyo, Japan).

Determination of glucose, lipids, and TNFα levels in the peripheral circulation

Blood was centrifuged at 4 °C in a sealed tube, and plasma glucose and TNF-α levels were then detected individually by the enzymatic colorimetric method and by TNF-α ELISA kit following the protocol of the kits (R&D Systems, Minneapolis, MN, USA). The serum triglyceride and total cholesterol levels were determined by enzymatic methods (kits, Zhong Sen Co., Beijing, People's Republic of China). High-density lipoprotein cholesterol (HDL-C) levels were determined after sodium phosphotungstate/magnesium chloride precipitation of low-density lipoprotein by polyvinyl sulfate.

Determination of disaccharidase activity in the jejunal mucosa

Jejunal samples were homogenized in ice-cold phosphate-buffered saline (PBS, pH 7.4). After centrifugation at 1,050×*g* for 15 min at 4 °C, the supernatant was used to measure maltase and sucrase activities with corresponding assay kits (Jiancheng Bio-Engineering Institute, Nanjing, People's Republic of China). Protein concentrations in homogenates were determined using a BCA Protein Assay Kit (Pierce Biotechnology, Inc., Rockford, IL, USA) according to the manufacturer's instructions.

Radioimmunoassay for SST levels in the jejunum and blood

The scraped jejunal mucosas were weighed and transferred to a boiling water bath for 5 min. They were then homogenized in 1.0 mL of 1 mol/L ice-cold acetic acid, left at 4 °C for 2 h, neutralized with 1.0 mL of 1 mol/L NaOH, and then centrifuged (4 °C, 15 min, 1,050×*g*). The supernatants were kept at −80 °C until analysis. Blood was obtained from the tail vein, mixed with 10 % EDTA-Na_2 60 μL, aprotinin 3,000 kIU, and immediately centrifuged (4 °C, 5 min, 1,050×*g*). The 0.5-mL plasma was transferred into 50 μL acetic acid in another tube. Two milliliters of 100 % acetone pre-cooled to 4 °C was added, and the mixture was centrifuged (4 °C, 15 min, 380×*g*) twice. The supernatants were collected, dried with a freeze dryer, and frozen at −80 °C until analysis. Supernatants were collected for the measurement of SST levels by an SST radioimmunoassay kit (RIA Technology Development Center, PLA General Hospital, Beijing, People's Republic of China) according to the manufacturer's instructions. Each specimen was measured in duplicate. Since octreotide, a synthetic octapeptide analog of SST, shares up to 11 amino acids with SST, the RIA could not distinguish between the two. In the preliminary test for SST measurement, octreotide was able to replace competitively the binding of ^{125}I-SST with its antibody. Thus, the total bindings for SST antibody in the plasma after octreotide injection were defined as SST–like immunoreactivity (SST–LIR).

Immunohistochemical staining of SGLT-1 and SST

Immunohistochemistry was performed on 5-μm paraffin-embedded tissue sections on poly-L-lysine-coated glass slides. The sections were deparaffinized and microwaved for 15 min. For nonspecific blocking, 10 % goat serum was added and sections were incubated for 20 min at 37 °C. Then, the following antibodies were added into individual sections: SGLT-1 goat anti-rat polyclonal antibody at a 1:200 dilution (Santa Cruz Biotechnology Inc., Santa Cruz, CA, USA) and SST antibody at a 1:100 dilution (Santa Cruz Biotechnology Inc., Santa Cruz, CA, USA). After being incubated overnight at 4 °C and rewarmed to 37 °C, the section was stained with a ready-to-use streptavidin–catalase immunohistochemical reagent system as a detection reagent. Color reactions were developed with 3,3′-diaminobenzidine (DAB; Zhongshan Bioagent Company, Beijing, People's Republic of China). A semiquantitative immunohistochemical analysis of raw data with Image-Pro Plus 4.0 software (Media Cybernetics, Silver Spring, MD, USA) was used to score integrated optical density (IOD) of positive reaction areas.

Quantification of SGLT-1 in the jejunal mucosa with reverse transcription polymerase chain reaction (RT–PCR) and Western blot analysis

Total RNA was extracted using Trizol reagent (Takara Bio-Engineering Co., Ltd., Kyoto, Japan) from the frozen jejunum samples. First-strand cDNA was synthesized from 2 μg of total RNA for each sample using reverse transcription kits (MBI, Fermentas Life Sciences Inc., Vilnius, Lithuania). The PCR primers were as follows [20]: SGLT-1 sense, 5′-CTT CTG GGG ACT GAT TCT CG-3′ and antisense, 5′-CGC TCT TCT GTG CTG TTA CG-3′; glyceraldehyde-3-phosphate dehydrogenase (GAPDH) sense, 5′-CAT GAC CAC AGT CCA TGC CA-3′ and antisense, 5′-CAC CCT GTT GCT GTA GCC ATA TTC-3′. PCR were catalyzed using Taq DNA polymerase (MBI, Fermentas Life Sciences Inc., Vilnius, Lithuania). The thermal cycling parameters consisted of an initial denaturation step for 5 min at 94 °C, followed by 23 cycles consisting of 1 min at 94 °C, 1 min at 60 °C, 1 min at 72 °C. The final extension step was for 7 min at 72 °C.

PCR products were resolved by 2 % agarose gel electrophoresis and visualized by ethidium bromide staining. Densitometry was carried out using a Bio-Rad GelDoc image acquisition system and Quantity One (v. 4.3) quantitation software (Bio-Rad, Hercules, CA, USA).

Protein was extracted from the scraped jejunal mucosa and measured with a BCA Protein Assay Kit (Pierce Biotechnology Inc., Rockford, IL, USA). The extracted protein (60 μg) was incubated in loading buffer and heated at 100 °C for 5 min. Samples were loaded onto an 10 % sodium dodecyl sulfate–polyacrylamide gel, then transferred electronically to polyvinylidene difluoride membranes (Millipore, Bedford, MA, USA). The membranes were incubated with a 1:1,000 dilution of rabbit polyclonal anti-SGLT-1 antibody (Millipore, Bedford, MA, USA) at 4 °C overnight. The membranes were then washed three times in blocking solution and incubated with secondary antibody (Santa Cruz Biotechnologies Inc., 1:50,000). The signals were developed using Super-Signal West Pico chemiluminescent substrate (Pierce Biotechnology Inc. Rockford, IL, USA). Band densities were quantified using Quantity One software 4.3.1 (Bio-Rad). Each value was expressed as the ratio of the IOD of the SGLT-1 band to that of GAPDH.

Statistical analysis

All data were analyzed using SPSS 13.0 statistical software (SPSS Inc., Chicago, IL, USA), and results are presented as mean ± SD. An ANOVA was used for all between-group comparisons. A p value ≤ 0.05 was considered significant.

Results

Nutritional states, plasma glucose, and serum lipid levels

In this study, we first made the animal model. After 24 weeks (168 days) of high-fat diet induction, the obese model was made successfully. The octreotide experiment then took 8 days. Therefore, we treated the rats for 176 days in total.

The weight of food intake was not significantly different among the three groups. The high-fat control and high-fat + octreotide groups had identical net energy intake. The rats in the high-fat control group showed typical features of obesity, such as elevated body weight, Lee's index, total fat weight and fat-to-body ratios, blood glucose, and serum TG and TC levels; their HDL-C levels were lower than those of the control group ($p < 0.01$). After 8 days' treatment with octreotide, all of the elevated values except Lee's index were significantly lower than those of the high-fat control group ($p < 0.05$ or $p < 0.01$). The decreased fat mass and fat-to-body ratios in the high-fat + octreotide group were similar to those of the normal control group ($p > 0.05$). Similar changes were observed in the glucose, triglyceride, and total cholesterol levels in circulation (Table 1). The HDL-C levels in the high-fat + octreotide group were tended to be increased compared to the high-fat control group; however, it did not reach to statistical significance ($p > 0.05$).

Morphological changes in intestinal villi and subcellular structures of epithelia

Both the height and quantity of intestinal villi in the high-fat control group were significantly higher (Fig. 1) than those of the normal controls ($p < 0.01$) (Table 1). After octreotide intervention, the height and quantity of intestinal villi were significantly lower than those of the high-fat control group ($p < 0.05$) and were similar to those of the normal controls ($p > 0.05$). There were no obvious differences in the crypt depth among three groups ($p > 0.05$) (Fig. 1; Table 1).

The high-fat control rats presented swollen mitochondria with fewer inner cristae and longer microvilli in the intestinal epithelia compared with the normal controls (Fig. 1). These abnormal changes in the mitochondria were reversed by octreotide treatment.

Disaccharidase activity in the intestinal mucosa

Maltase activity in the intestinal mucosa of the high-fat control group was about 2.6-fold higher than that in the normal control group ($p < 0.01$). The octreotide group's maltase activity was much lower than that of the high-fat control group ($p < 0.05$) and was similar to that of the normal control group ($p > 0.05$) (Table 1). There were no significant differences in sucrase activity among three groups ($p > 0.05$) (Table 1).

Expression of SGLT-1 in the jejunal mucosa

The mRNA expression of SGLT-1 in the high-fat control group was significantly higher than that in the normal control rats ($p < 0.05$). The expression level was significantly lower in the high-fat + octreotide group than in the high-fat control animals ($p < 0.05$) (Fig. 2).

Immunohistochemistry and Western blot showed that SGLT-1, mainly located in the brush border of the intestinal villi, was over-expressed in the high-fat control group ($p < 0.01$) (Fig. 3). Its expression in the high-fat + octreotide group was significantly lower by comparison ($p < 0.01$) and similar to that of the normal controls ($p > 0.05$).

SST and SST–LIR levels in intestinal mucosa and plasma

Immunohistochemistry showed that the expression of SST in the intestinal mucosa of the high-fat control rats was

Table 1 The changes in parameters in three groups

	Control ($n = 18$)	High-fat control ($n = 19$)	High-fat + octreotide ($n = 21$)
Obese states			
Body weight (g)	378.5 ± 111.75	605.6 ± 141.00**	508.8 ± 94.39**,▲
Fat weight (g)	15.94 ± 14.65	45.00 ± 28.84**	21.69 ± 15.35▲▲
Fat/body weight ratio (%)	3.74 ± 2.95	7.66 ± 3.24**	4.02 ± 2.10▲▲
Lee index	318.73 ± 20.10	337.57 ± 10.82**	334.67 ± 22.13*
Plasma glucose (mmol/L)	7.33 ± 0.70	8.60 ± 1.38**	7.58 ± 1.51▲
Serum lipids levels(mmol/L)			
Triglyceride	0.96 ± 0.21	1.45 ± 0.34**	1.12 ± 0.27▲▲
Total cholesterol	1.74 ± 0.38	2.02 ± 0.30*	1.71 ± 0.32▲▲
HDL-C	1.00 ± 0.18	0.88 ± 0.14*	0.98 ± 0.19
Jejunal absorptive area			
Villus height (μm)	311 ± 87.06	423 ± 102.06**	340 ± 83.25▲
Crypt depth (μm)	169 ± 36.29	179 ± 25.11	171 ± 24.43
Number of villi/field	23.6 ± 3.41	30.7 ± 4.19**	25.5 ± 1.76▲
SST or SST–LIR levels (radioimmunoassay)			
Intestinal (pg/mg)	356.39 ± 146.78	231.12 ± 98.18*	480.01 ± 286.65▲
Plasma (pg/mL)	129.56 ± 47.36	117.77 ± 58.34	184.45 ± 99.75*,▲
Plasma TNF-α (pg/mL)	10.45 ± 1.23	13.43 ± 0.87*	11.27 ± 1.01▲
Activity of disaccharidase (U/mg protein)			
Maltase	50.43 ± 30.49	129.56 ± 71.57**	63.95 ± 62.94▲
Sucrase	53.84 ± 17.98	50.18 ± 14.13	46.95 ± 20.72
Food intake			
Net energy (kcal/day/rat)	86.5 ± 17.47	126.7 ± 18.92**	121.5 ± 15.66**
Energy in chow (kcal/g)	2.90	4.30**	4.30**
Chow (g/day/rat)	29.8 ± 6.0	29.5 ± 4.4	28.2 ± 3.7

* $p < 0.05$; ** $p < 0.01$ versus control group

▲ $p < 0.05$; ▲▲ $p < 0.01$ versus high-fat control group

markedly lower than that of the normal control group. The difference was quantified by RIA at about 54 % ($p < 0.05$) (Table 1). Compared with the high-fat control rats, those treated with octreotide had significantly enhanced SST–LIR levels in their intestinal mucosa ($p < 0.05$) (Fig. 4). SST and SST–LIR levels in the plasma of the three groups showed a similar pattern (Table 1).

Plasma levels of TNF-α

Compared with the normal control group, the plasma levels of TNF-α in the high-fat control rats were significantly higher ($p < 0.05$). However, the octreotide-treated rats had much lower levels than the high-fat controls ($p < 0.05$); their TNF-α levels were similar to those of the normal controls ($p > 0.05$) (Table 1).

Discussion

Obesity results from disruption of the homeostasis between food intake and energy expenditure, and the factors affecting these processes are the focus of extensive research. Since obesity-related metabolic disorders are characterized by low-grade inflammation of unknown molecular origin [21, 22], many prior studies have focused on adipocytes as sources of inflammatory mediators in obesity [23–27]. Recently, low-grade inflammation has emerged as an early consequence of a high-fat diet and as a possible contributor to obesity or associated insulin resistance. However, the link between low-grade intestinal inflammation and energy homeostasis is still obscure.

Low-grade inflammation is usually characterized by higher portal plasma LPS levels and inflammatory tone (i.e., an increase in circulating cytokines, such as TNF-α and interleukin (IL)-6, -10, and -15) [7, 28]. Accordingly, the higher plasma TNF-α level in the rats fed a high-fat diet in this study indicated low-grade inflammation. Morphologically, the jejunal mucosa of those rats did not display chronic inflammation under the microscope, but the swollen mitochondria in their jejunal epithelia may imply chronic inflammatory injury to the intestine [29, 30]. Our previous experiment observed that either acute or chronic intestinal inflammation with high levels of cytokines, including TNF-α and IFN-γ, was always associated with low SST levels in the intestinal mucosa due to the

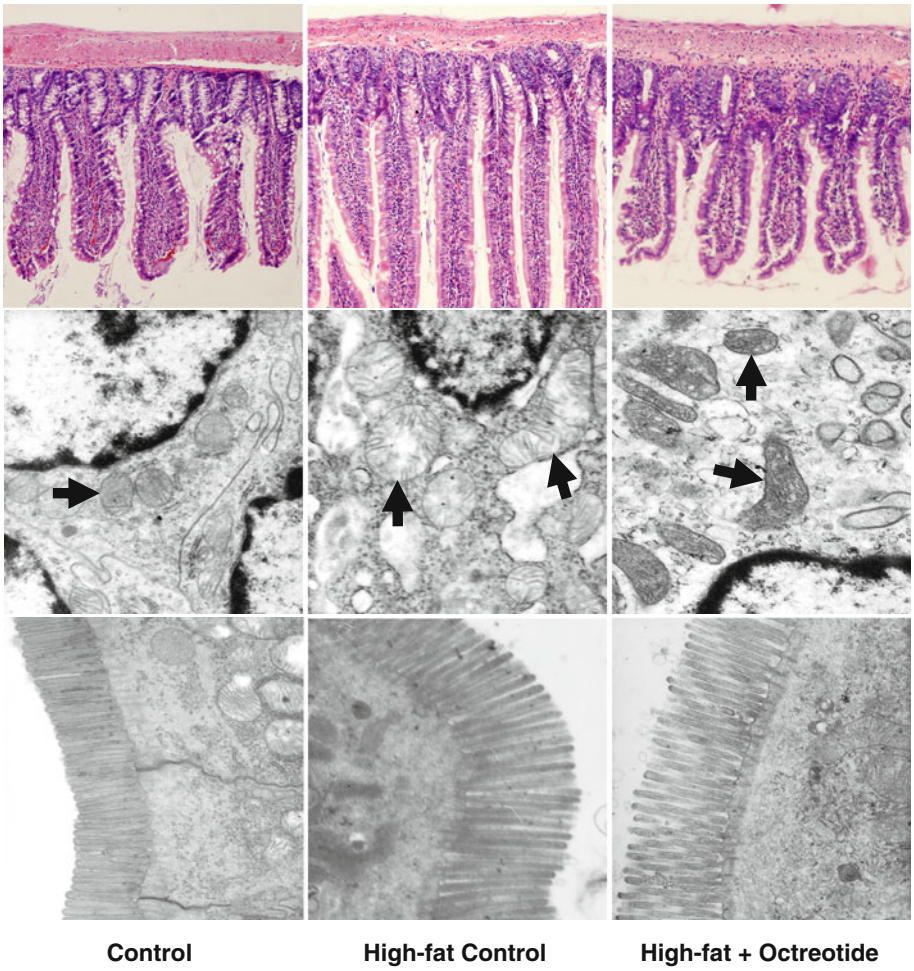

Fig. 1 Morphological changes in intestinal villi and subcellular structures of epithelia. *1st line* Histological sections showed longer and more numerous intestinal villi in the high-fat control rats (hematoxylin and eosin stain, magnification $\sim \times 200$). *2nd line* Transmission electron microscopy revealed swollen mitochondria (*arrowed*) in the high-fat control rats. Octreotide greatly reversed the changes in the mitochondria (*arrowed*, magnification $\sim \times 17{,}000$). *3rd line* Longer epithelial microvilli were evident in the high-fat control rats (magnification $\sim \times 15{,}000$)

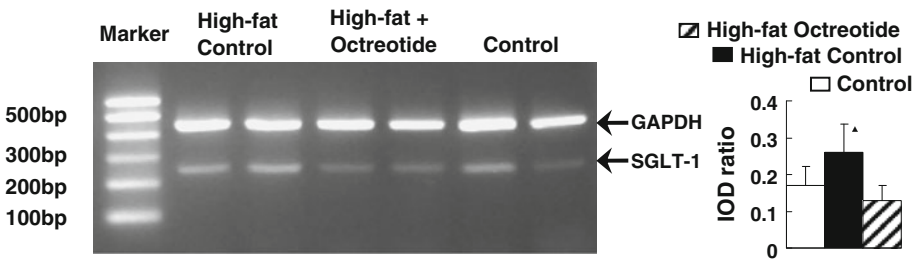

Fig. 2 mRNA expression for intestinal SGLT-1 (RT–PCR). The greatly increased IOD ratio of intestinal SGLT-1/GAPDH in the high-fat control rats compared with the control rats fell significantly in the high-fat + octreotide rats, $^{\blacktriangle}p < 0.05$. Each value represents the mean ± SD for all animals in the corresponding group (duplicate measurements were made)

impairment of entero-SST production [13, 29]. This inverse correlation between TNF-α and intestinal SST was again found and quantified in the present study's high-fat diet-induced rat model. Small intestinal crypt cell proliferation is essential to the normal renewal of the epithelium. Another group has reported that SST may inhibit the growth of rat crypt cells at an upstream site during the cellular growth response [17]. Loss of this negative regulation for intestinal epithelial growth of SST in low-grade inflammation may promote cell proliferation in the mucosa and greatly increase the height and quantity of jejunal villi. The enlarged absorption area of jejunum would favor the entry of nutrients into the organism, contributing to the development of obesity.

Apart from altering the architecture of the jejunal villi, high-fat diet also increased the maltase activity of the rats 2.6-fold, enhancing their capacity to digest carbohydrate. Normally, amylase cleaves starch into disaccharide units, such as maltose and sucrose, that further split into monosaccharides such as glucose, galactose, and fructose. The

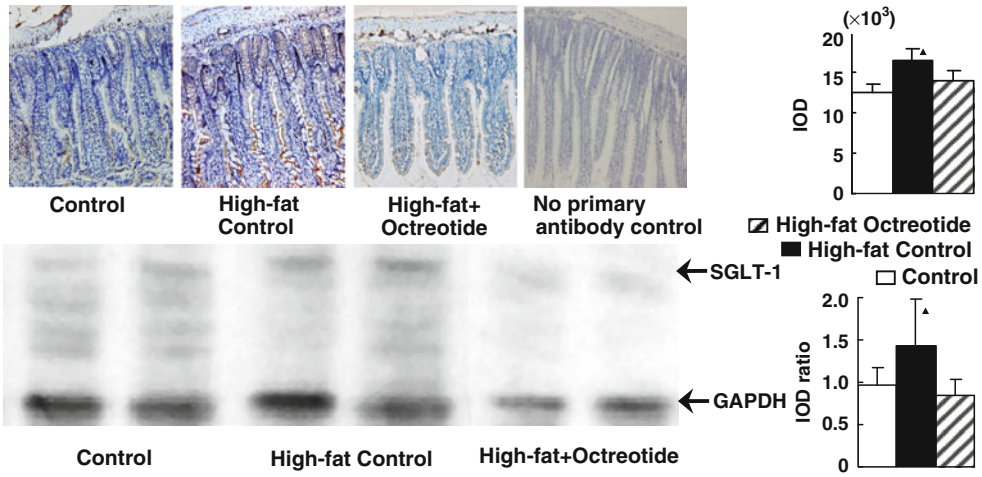

Fig. 3 Protein expression of intestinal SGLT-1. *1st line* Positive expression of SGLT-1 manifests as brown granules. Samples not treated with primary antibody were used as negative controls. Immunohistochemical stain, magnification $\sim \times 200$. *2nd line* Intestinal expression of SGLT-1/GAPDH was quantified by Western blot. SGLT-1 expression in the high-fat control rats, whether detected by immunohistochemistry or by Western blot, was significantly higher than those of both the control and high-fat + octreotide rats, $^{\blacktriangle}p < 0.05$. Each value represents the mean ± SD for all animals in the corresponding group (duplicate measurements were made)

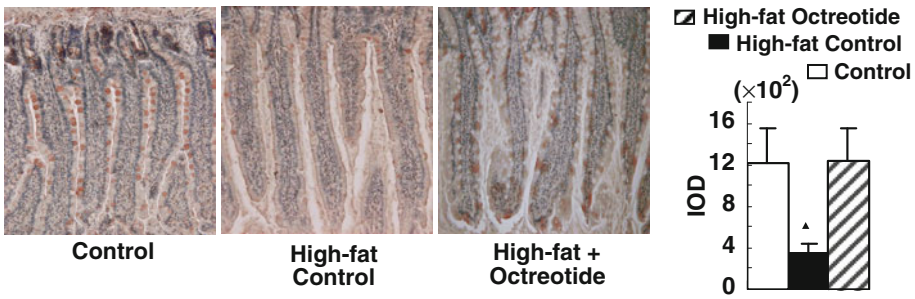

Fig. 4 SST or SST–LIR expression in the intestinal mucosa (radioimmunoassay). Positive expression of SST or SST–LIR appeared as *brown granules* (immunohistochemical stain, magnification $\sim \times 200$). The expression of SST was dramatically lower in the high-fat control rats compared with the normal control rats, $^{\blacktriangle}p < 0.05$, while those treated with octreotide had significantly enhanced SST–LIR levels compared with the high-fat control rats, $^{\blacktriangle}p < 0.05$. Each value represents the mean ± SD for all animals in the corresponding group (duplicate measurements were made)

activity of disaccharidases usually depends on the concentration of their substrate in the jejunal lumen [31, 32]. To ensure the establishment of an obese rat model in this study, some sucrose was added to the rats' high-fat diet. However, sucrase activity was not enhanced in those rats. This may be explained by an observation by Black et al. [33] that high-fat diet could stimulate the secretion of trypsin, which may degrade sucrase molecules.

Glucose absorption in the small intestine is essential for carbohydrate energy supply. This absorption is mediated by two transporters in the enterocytes: SGLT-1 in the brush border membrane and the sodium-independent glucose transporter GLUT2 in the basolateral membrane [34]. SGLT-1 expression may be related to either the trophic villi or high levels of plasma TNF-α, which appear to up-regulate SGLT-1 expression by inhibiting the protein kinase C (PKC) signaling pathway [35]. Thus, the enlarged jejunum absorption area, higher maltase activity, and increased glucose absorption by SGLT1 in the rats fed with high-fat diet may have contributed to their excess caloric intake, development of several metabolic disorders, and high fat storage.

After obese rats were injected with octreotide for 8 days, their intestinal SST–LIR level increased and plasma TNF-α fell significantly. Mitochondrial dilation was also attenuated. The greatly decreased jejunum absorption area, maltase activity, and SGLT-1 expression in these rats apparently reduced the intestinal absorption of energy nutrients. The rats' metabolic disorders and fat storage were then alleviated. All of these data provide further evidence that low-grade intestinal inflammation is involved in the deposit of energy in fat, and reveal a previously unrecognized role of octreotide in the treatment for diet-induced obesity.

There is a limitation of this study. We only included the normal diet control, high-fat control, and high-fat octreotide groups in this study. Additional placebo groups given subcutaneous injections with saline or vehicle for octreotide would rule out a possible effect accounting on stress associated with subcutaneous injections for the animals.

In summary, we have elucidated a new pathophysiological mechanism linking low-grade inflammation induced by high-fat diet to increased intestinal absorption of energy nutrients and adipose tissues via reduced intestinal SST production. Octreotide treatment may effectively reverse such disorders, which would have far-reaching significance for regulating energy balance.

Acknowledgments This work was supported by grants from the National Natural Sciences Foundation of China (No. 30870919) and Sichuan Provincial Department of Science and Technology (No. 2010SZ0176).

Conflict of interest The authors declared no conflict of interest.

References

1. Van der Merwe MT (2009) Obesity in women-a life cycle of medical risk. JEMDSA 14:139–142
2. Livhits M, Mercado C, Yermilov I, Parikh JA, Dutson E, Mehran A, Ko CY, Gibbons MM (2010) Behavioral factors associated with successful weight loss after gastric bypass. Am Surg 76: 1139–1142
3. Atkinson RL (2005) Management of obesity: pharmacotherapy. In: Kopelman PG, Caterson LD, Dietz WH (eds) Clinical obesity in adults and children. Blackwell, Malden, pp 380–393
4. Cordido F, Isidro ML (2010) Approved and off-label uses of obesity medications and potential new pharmacologic treatment options. Pharmaceuticals 3:125–145
5. Lustig RH, Hinds PS, Ringwald-Smith K, Christensen RK, Kaste SC, Schreiber RE, Rai SN, Lensing SY, Wu S, Xiong X (2003) Octreotide therapy of pediatric hypothalamic obesity: a double-blind, placebo-controlled trial. J Clin Endocrinol Metab 88: 2586–2592
6. Caesar R, Fåk F, Bäckhed F (2010) Effects of gut microbiota on obesity and atherosclerosis via modulation of inflammation and lipid metabolism. J Intern Med 268:320–328
7. Muccioli GG, Naslain D, Bäckhed F, Reigstad CS, Lambert DM, Delzenne NM, Cani PD (2010) The endocannabinoid system links gut microbiota to adipogenesis. Mol Syst Biol 6:392
8. Brignardello J, Morales P, Diaz E, Romero J, Brunser O, Gotteland M (2010) Pilot study: alterations of intestinal microbiota in obese humans are not associated with colonic inflammation or disturbances of barrier function. Aliment Pharmacol Ther 32: 1307–1314
9. Mansford KRL (1967) Recent studies on carbohydrates absorption. Proc Nutr Soc 26:27–34.doi:10.1079/PNS19670008
10. Dyer J, Daly K, Salmon KS, Arora DK, Kokrashvili Z, Margolskee RF, Shirazi-Beechey SP (2007) Intestinal glucose sensing and regulation of intestinal glucose absorption. Biochem Soc Trans 35:1191–1194
11. Ahlman H, Nilsson O (2001) The gut as the largest endocrine organ in the body. Ann Oncol 12(Suppl 2):S63–S68
12. Tang C, Lan C, Wang CH, Liu R (2005) Alleviation of multiple organ dysfunction syndrome by somatostatin via suppression of intestinal mucosal mast cells. Shock 23:470–475
13. Wu H, Liu L, Tan QH, Wang CH, Guo MM, Xie YM, Tang CW (2009) Somatostatin limits intestinal ischemia-reperfusion injury in macaques via suppression of TLR4–NF-κB cytokine pathway. J Gastrointestinal Surg 13:983–993
14. Pintér E, Helyes Z, Szolcsányi J (2006) Inhibitory effect of somatostatin on inflammation and nociception. Pharmacol Ther 112:440–456
15. Csaba Z, Dournaud P (2001) Cellular biology of somatostatin receptors. Neuropeptides 35:1–23
16. Guo MM, Tan QH, Fan H, Huang MH, Wang CH, Qiu XQ, Tang CW (2005) Changes of somatostatin and expression of somatostatin receptor in small intestine and liver tissues during macaque development. Acta Physiol Sin 57:719–724
17. Hodin RA, Saldinger P, Meng S (1995) Small bowel adaptation: counter regulatory effects of epidermal growth factor and somatostatin on the program of early gene expression. Surgery 118:206–210; discussion 210–211
18. Wang ZX, Chen JW, Zhou YK (2002) An experimental study of the effects of octreotide on small intestinal mucosa in rats. J Math Med 15:125–127 (article in Chinese)
19. Silva AP, Bethmann K, Raulf F, Schmid HA (2005) Regulation of ghrelin secretion by somatostatin analogs in rats. Eur J Endocrinol 152:887–894
20. Kang L, Routh VH, Kuzhikandathil EV, Kuzhikandathil EV, Gaspers LD, Levin BE (2004) Physiological and molecular characteristics of rat hypothalamic ventromedial nucleus glucosensing neurons. Diabetes 53:549–559
21. Hotamisligil GS, Erbay E (2008) Nutrient sensing and inflammation in metabolic diseases. Nat Rev Immunol 8:923–934
22. Shoelson SE, Goldfine AB (2009) Getting away from glucose: fanning the flames of obesity-induced inflammation. Nat Med 15:373–374
23. Kern PA, Ranganathan S, Li C, Wood L, Ranganathan G (2001) Adipose tissue tumor necrosis factor and interleukin-6 expression in human obesity and insulin resistance. Am J Physiol Endocrinol Metab 280:E745–E751
24. Syrenicz A, Garanty-Bogacka B, Syrenicz M, Gebala A, Walczak M (2006) Low grade systemic inflammation and the risk of type 2 diabetes in obese children and adolescents. Neuro Endocrinol Lett 27:453–458
25. Panagiotakos DB, Pitsavos C, Yannakoulia M, Chrysohoou C, Stefanadis C (2005) The implication of obesity and central fat on markers of chronic inflammation: the ATTICA study. Atherosclerosis 183:308–315
26. Visser M, Bouter LM, McQuillan GM, Wener MH, Harris TB (2001) Low grade systemic inflammation in overweight children. Pediatrics 107:E13
27. Dandona P, Weinstock R, Thusu K, Abdel-Rahman E, Aljada A (1998) Tumor necrosis factor-alpha in sera of obese patients: fall with weight loss. J Clin Endocrinol Metab 83:2907–2910
28. Lee YH, Pratley RE (2005) The evolving role of inflammation in obesity and the metabolic syndrome. Curr Diab Rep 5:70–75
29. Zhou C, Li J, Wang HY, Tang CW (2009) Decreased somatostatin is related to the hypersensitivity of intestinal epithelia to LPS via up–regulated TLR4–TBK1 pathway in rats chronically exposed to ethanol. Alcohol 43:293–303
30. Joshi MS, Crouser ED, Julian MW, Schanbacher BL, Bauer JA (2000) Digital imaging analysis for the study of endotoxin-induced mitochondrial ultrastructure injury. Anal Cell Pathol 21:41–48
31. Rosensweig NS (1975) Diet and intestinal enzyme adaptation: implications for gastrointestinal disorders. Am J Clin Nutr 28:648–655

32. Ferraris RP, Villenas SA, Diamond J (1992) Regulation of brush-border enzyme activities and enterocyte migration rates in mouse small intestine. Am J Physiol Gastrointest Liver Physiol 262: G1047–G1059
33. Black BL, Croom J, Eisen EJ, Petro AE, Edwards CL, Surwit RS (1998) Differential effects of fat and sucrose on body composition in A/J and C57BL/6 mice. Metabolism 47:1354–1359
34. Hediger MA, Rhoads DB (1994) Molecular physiology of sodium glucose cotransporters. Physiol Rev 74:993–1026
35. Lee JY, Hannun YA, Obeid LM (2000) Functional dichotomy of protein kinase C (PKC) in tumor necrosis factor-a (TNF-α) signal transduction in L929 cells. J Biol Chem 275:29290–29298